

Unusual scaling for pulsed laser deposition

Berit Hinnemann¹, Haye Hinrichsen², and Dietrich E. Wolf¹

¹ *Theoretische Physik, Fachbereich 10, Gerhard-Mercator-Universität Duisburg, 47048 Duisburg, Germany*

² *Theoretische Physik, Fachbereich 8, Universität GH Wuppertal, 42097 Wuppertal, Germany*

(January 22, 2001)

We demonstrate that a simple model for pulsed laser deposition exhibits an unusual type of scaling behavior for the island density in the submonolayer regime. This quantity is studied as function of pulse intensity and deposition time. We find a data collapse for the *ratios of the logarithms* of these quantities, whereas conventional scaling as observed in molecular beam epitaxy involves ratios of powers.

PACS numbers: 64.60.Ht, 68.55.Ac, 81.15.Fg

Many systems in equilibrium and nonequilibrium statistical physics exhibit power-law scaling. This means that a system with an observable, M , depending for example on two parameters, z_1 and z_2 , looks the same, if the units of M , z_1 and z_2 are rescaled by certain factors which are related to each other by power-laws. Such a scaling transformation can be written as

$$z_1 \rightarrow \Lambda z_1, \quad z_2 \rightarrow \Lambda^\beta z_2, \quad M \rightarrow \Lambda^\alpha M, \quad (1)$$

where Λ is a scaling parameter and α, β are certain exponents. Eq. (1) implies the scaling form

$$M(z_1, z_2) = z_1^\alpha f(z_2/z_1^\beta), \quad (2)$$

where f is a scaling function depending on a scale-invariant argument. This type of scaling can be observed in a vast variety of applications, including equilibrium critical phenomena [1,2], growth processes [3–8], driven diffusive systems [9], as well as phase transitions far from equilibrium [10,11].

The main theoretical interest in power-law scaling stems from the fact that the long-range properties of such systems are universal, i.e., they are determined by certain symmetry properties and do not depend on microscopic details of the dynamics. This allows one to categorize phase transitions and growth phenomena into universality classes. Typically each universality class is associated with a certain set of values of the critical exponents. Moreover, the functional form of the scaling function f turns out to be universal as well.

As an example for power-law scaling, which we are going to contrast with a different type of scaling in this paper, let us consider the following well-known simple model of molecular beam epitaxy (MBE): A particle beam deposits atoms onto a flat substrate at a flux F (atoms per unit area per unit time). The atoms diffuse on the substrate with a surface diffusion constant D until they meet another adatom, in which case they form a stable and immobile nucleus of a two-dimensional island on the surface, or until they attach irreversibly to the edge of an already existing island. If they reach the edge diffusing on top of the island, they go down and attach

to the edge with the same probability as if they arrived there from the lower terrace, i.e., Ehrlich-Schwoebel barriers are not taken into account.

The observable examined in this paper is the time-dependent nucleation density, n , i.e., the number of nucleation events per unit area in the first layer integrated over time. Obviously, the nucleation density is a fundamental quantity characterizing the island morphology as it indicates how many islands are formed. By definition, the nucleation density increases monotonically with time and saturates at a constant value when the first monolayer is completed.

In MBE the two parameters D and F can be used to construct a characteristic length

$$\ell_0 = (D/F)^{1/4}. \quad (3)$$

When the nucleation density reaches the value $1/\ell_0^2$, the rate of nucleation events decreases drastically since it becomes more likely that an adatom attaches to an already existing island instead of meeting another adatom and forming a nucleus. In terms of the coverage $\Theta = Ft$, i.e., the total number of deposited atoms per unit area, the time dependence of n is known to obey the scaling form

$$n(\ell_0, \Theta) = \ell_0^{-2} f(\Theta \ell_0^2). \quad (4)$$

As shown in Ref. [12], the scaling function f behaves as

$$f_1(z) \propto \begin{cases} z^3 & \text{for } 0 \leq z \ll 1 \\ z^{1/3} & \text{for } 1 \ll z \ll \ell_0^2/a^2 \end{cases}, \quad (5)$$

where a is the lattice constant, which will be set to unity. Thus, MBE exhibits standard power-law scaling as described by Eqs. (1) and (2). However, in pulsed laser deposition (PLD), an alternative method of growing thin epitaxial films, we find that the nucleation density shows a fundamentally different type of scaling, which in MBE is realized only approximately.

In order to work out the difference most clearly, let us assume that the amplitudes of the asymptotic power laws in (5) are equal (which is approximately the case in MBE), so that one can get rid of them by dividing

$n(\ell_0, \Theta)$ by the nucleation density at a particular coverage Θ_0 . In the following we choose $\Theta_0 = 1$ and define

$$M(\ell_0, \Theta) = n(\ell_0, \Theta)/n(\ell_0, 1) = \ell_0^{-2/3} f_2(\Theta \ell_0^2). \quad (6)$$

The scaling function f_2 is obtained from f_1 by replacing the proportionality in (5) by an equal-sign. If we furthermore suppose that the asymptotic power laws in (5) would remain valid right to the crossover point at $\Theta \ell_0^2 = 1$ (which is certainly not the case), then the scaling function would have the additional symmetry

$$f_2(z^\lambda) = f_2^\lambda(z). \quad (7)$$

As a consequence the system would not only be invariant under the scale transformation (1),

$$\ell_0 \rightarrow \Lambda \ell_0, \quad \Theta \rightarrow \Lambda^{-2} \Theta, \quad M \rightarrow \Lambda^{-2/3} M, \quad (8)$$

but also under

$$\ell_0 \rightarrow \ell_0^\lambda, \quad \Theta \rightarrow \Theta^\lambda, \quad M \rightarrow M^\lambda. \quad (9)$$

This is a scaling transformation for the *logarithms* with all critical exponents equal to 1. According to (2) this would imply

$$\ln M = (\ln \ell_0) g(\ln \Theta / \ln \ell_0). \quad (10)$$

with a piecewise linear scaling function $g(z)$ whose slopes are determined by the exponents in (5).

While in MBE this type of scaling holds only in an approximate sense, we are going to show that PLD indeed obeys this scaling form with a *quadratic* scaling function g . PLD is a growth technique in which the target material is ablated by a pulsed laser and then deposited in pulses on a substrate surface, i.e., many particles arrive simultaneously at the surface [13]. Experimentally each pulse has a length of about a few nanoseconds and the time between two pulses is of the order of seconds. In order to investigate the scaling behavior of PLD, we consider a simple model which generalizes the standard model for MBE [14,15]. In this model the duration of a pulse is assumed to be zero and the transient enhancement of the mobility of freshly deposited atoms is neglected. It is controlled by three parameters, namely, the intensity, I , which is the density of particles deposited per pulse, the rate for diffusion of adatoms on the surface, D , and the average flux of incident particles per site, F . Since there is no edge diffusion, the islands grow in a fractal manner before they coalesce. A similar model with a finite pulse length was studied previously by Jensen, Niemeyer, and Combe [16,17].

If the intensity I is very low, PLD and MBE display essentially the same properties. However, if the intensity exceeds the average density of adatoms during a MBE process, we expect a crossover to a different type of behavior. Since this density is known to scale as

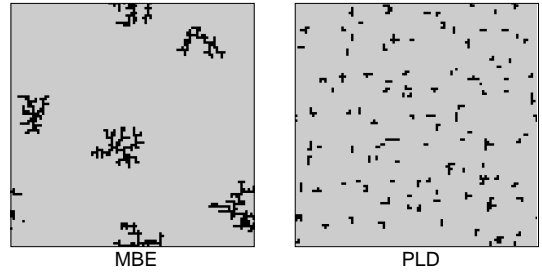


FIG. 1. Molecular beam epitaxy (left) compared to pulsed laser deposition (right) for $D/F = 10^8$ and $I = 0.01$. The figure shows typical configurations after deposition of 0.05 monolayers.

$(D/F)^{1-2\gamma}$, where $\gamma = 1/(4 + d_f) \simeq 1/6$, the crossover takes place at a critical intensity

$$I_c \approx (D/F)^{-2/3}. \quad (11)$$

The qualitative difference between PLD and MBE for $I > I_c$ is shown in Fig. 1. As can be seen, there are much more nucleations at an early stage, although the effective flux of incoming particles is the same in both cases.

In order to avoid the influence of the crossover at $I \approx I_c$, we restrict our PLD-simulations to a particularly simple case, namely to the limit of an infinite D/F , meaning that all adatoms nucleate or attach to an existing island before the next pulse arrives. In this limit $I_c = 0$, and the nucleation density again depends only on two variables, $n(I, \Theta)$.

Performing Monte Carlo simulations we investigated the nucleation density for various intensities using a system size of 400×400 . The measurement always takes place right before a new pulse is released. Our results are shown in Fig. 2. As can be seen, $n(I, \Theta)$ increases with increasing intensity I . This is plausible since for a higher intensity more atoms arrive at the surface simultaneously so that most of them can meet and form new nucleations before attaching to already existing islands.

Obviously, the curves in Fig. 2 do not display asymptotic power laws, rather they are defined on finite intervals. Moreover, it is impossible to produce an ordinary data collapse by shifting the curves horizontally and vertically in the double-logarithmic plot. Thus, the usual scaling theory relying on power-law scaling fails. However, as we are going to show below, it is possible to generate a data collapse by using the scaling form (10).

The main idea is to stretch the curves in Fig. 2 both horizontally and vertically in such a way that their end-points collapse. To this end let us first consider the right-most data point of each curve. As shown in Ref. [14,15] the saturated nucleation density $n(I, 1)$ scales as

$$n(I, 1) \sim I^{2\nu}, \quad (12)$$

where the exponent ν was estimated numerically by

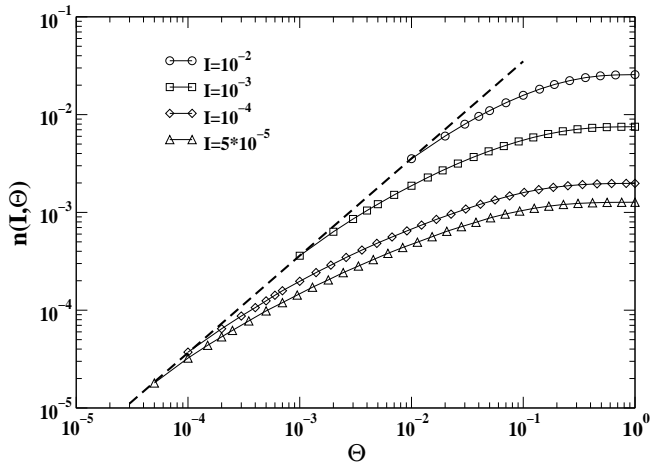


FIG. 2. The nucleation density versus time during the deposition of a monolayer. The dashed line has the slope 1.

$\nu \simeq 0.28(1)$. The rightmost points can be collapsed by plotting the normalized nucleation density

$$M(I, \Theta) = \frac{n(I, \Theta)}{n(I, 1)}. \quad (13)$$

against Θ , as shown in Fig. (3).

Turning to the leftmost data points in Fig. (2), which correspond to the measurements after the first pulse, we note that these points lie on a straight line with slope 1. This observation can be explained as follows. After deposition of the first pulse, the adatoms diffuse until they meet and nucleate. Most of them will nucleate with another adatom and form an island consisting of two atoms. Thus, after completion of the nucleation process, the nucleation density would be $I/2$. In reality, however, some of the adatoms form bigger islands with three or more particles, but to leading order these processes can be neglected. Thus, we can conclude that

$$n(I, I) \sim I \quad (14)$$

which is the vertical coordinate of the leftmost data points. Moreover, their horizontal coordinate of the points is given by $\Theta = I$, explaining the slope 1 of the dashed line in Fig. 2. In fact, the simulation data deviate from a linear law by less than 3 %.

Surprisingly the power laws (12) and (14) are valid not only for small I but also for $I \rightarrow 1$. This implies that the prefactors of (12) and (14) have to be identical. This can be seen from Fig. 3, where we plotted the normalized nucleation density $M(I, \Theta)$ versus Θ . In this representation the leftmost points of the curves obey a power law

$$M(I, I) \sim I^{1-2\nu} \quad (15)$$

extrapolating to $M(1, 1) = 1$, which proves the equality of the prefactors in Eqs. (12) and (14).

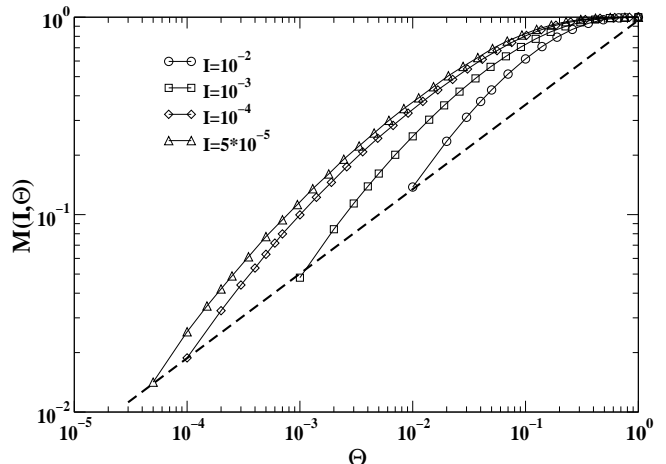


FIG. 3. The same data rescaled in such a way that all curves terminate at the point (1, 1).

After collapsing the rightmost data points, we collapse the leftmost data points by stretching the curves vertically and horizontally. This can be done by dividing $\ln M$ and $\ln \Theta$ by certain factors which are proportional to $1/\ln I$. Clearly, this manipulation does not affect the upper terminal point of the curves. In fact, plotting $\ln M/\ln I$ versus $\ln \Theta/\ln I$ (see Fig. 4), we obtain a convincing data collapse [18].

Assuming this data collapse to hold, the system turns out to be invariant under the transformation

$$M \rightarrow M^\lambda, \quad I \rightarrow I^\lambda, \quad \Theta \rightarrow \Theta^\lambda. \quad (16)$$

which implies the scaling form

$$\ln M \simeq (\ln I) g\left(\frac{\ln \Theta}{\ln I}\right). \quad (17)$$

This scaling form has the same structure as the approximate scaling law (10) for MBE. Moreover, we find that the scaling function is well approximated by a simple parabola

$$g(z) = a z^2, \quad (18)$$

so that $\ln M \simeq a \ln^2 \Theta / \ln I$. Because of the quadratic form the data collapse can be generated in several ways, e.g., by plotting $\ln M$ versus $\ln \Theta / \sqrt{\ln I}$.

Finally, we present a numerical puzzle. As outlined before, the scaling form (17) for PLD should also hold for finite D/F provided that $I \geq I_c$. Therefore, this scaling form can be compared with the approximate scaling form for MBE (10) at the crossover point $I \simeq I_c$, where both scaling concepts should ‘intersect’. Because of Eqs. (3) and (11), the system is then characterized by the length scale $\ell_0 \sim I^{-3/8}$. Consequently, the asymptotic power laws for MBE translated into the language of PLD read

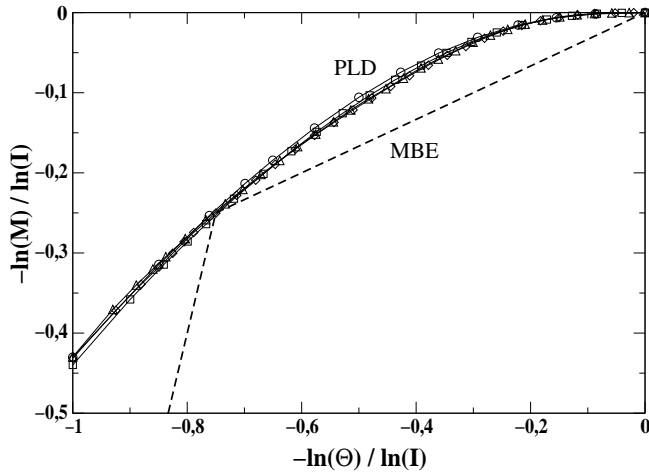


FIG. 4. Data collapse according to the scaling form (17).

$$M(I, \Theta) \simeq \begin{cases} \Theta^3/I^2 & \text{for } 0 < \Theta \ll I^{3/4} \\ \Theta^{1/3} & \text{for } I^{3/4} \ll \Theta \ll 1 \end{cases} \quad (19)$$

Taking the logarithm and dividing by $\ln I$ we obtain

$$\frac{\ln M(I, \Theta)}{\ln I} = \begin{cases} 3 \frac{\ln \Theta}{\ln I} - 2 & \text{for } \frac{3}{4} \ll \frac{\ln \Theta}{\ln I} \\ \frac{\ln \Theta}{3 \ln I} & \text{for } 0 \ll \frac{\ln \Theta}{\ln I} \ll \frac{3}{4} \end{cases} \quad (20)$$

In the limit $I \rightarrow 0$ the crossover between the two power laws becomes sharper so that Eq. (20) converges to a piecewise linear curve, which is shown in Fig. 4 as a dashed line. Surprisingly, the crossover point

$$\frac{\ln \Theta_c}{\ln I} = 3/4, \quad \frac{\ln M(I, \Theta_c)}{\ln I} = 1/4 \quad (21)$$

seems to lie precisely on the collapsed curves for PLD. If this were true, the prefactor a in Eq. (18) would be given by $a = 4/9$. Furthermore, the scaling relation (15) implies that the prefactor a and the exponent ν are related by $a = 1 - 2\nu$. Thus, we obtain the result

$$\nu = (1 - a)/2 = 5/18 \simeq 0.278. \quad (22)$$

Surprisingly, this value is in perfect agreement with the previous numerical estimate $\nu \simeq 0.28(1)$ of Ref. [15].

To summarize, we have demonstrated that a simple model for pulsed laser deposition displays an unusual type of scaling behavior. In its most general setup, this kind of scaling behavior is observed in systems which are invariant under the transformation

$$M \rightarrow M^{\lambda^\alpha}, \quad z_i \rightarrow z_i^{\lambda^{\beta_i}}, \quad (23)$$

for arbitrary λ , where α and β_1, \dots, β_n are certain exponents. The corresponding scaling form reads

$$\ln M \sim (\ln z_1)^\alpha g\left(\frac{\ln z_2}{(\ln z_1)^{\beta_2}}, \dots, \frac{\ln z_n}{(\ln z_1)^{\beta_n}}\right). \quad (24)$$

Performing numerical simulations, we have demonstrated that such a scaling form leads to a convincing data collapse for PLD in the limit of an infinite diffusion constant. In contrast to ordinary scaling functions the function g is defined on a limited interval between two points.

Various questions remain open. First of all, it would be nice to find further examples for this kind of scaling. In this context it would be particularly interesting to investigate an exactly solvable model with such a scaling behavior and to prove the validity of the proposed scaling form. Moreover, it is not yet clear to what extent the scaling function g is universal, i.e., independent of details of the dynamic rules of the model. Finally, the numerical coincidence of the crossover point (21) and a particular point of the collapsed curves is not yet understood.

We thank the Deutsche Forschungsgemeinschaft for support within SFB 491.

-
- [1] D. J. Amit, *Field Theory, the Renormalization Group, and Critical Phenomena*, World Scientific, Singapore (1984).
 - [2] T. M. Liggett, *Interacting Particles Systems*, Springer, Berlin (1985).
 - [3] S. F. Edwards and D. R. Wilkinson, Proc. R. Soc. Lond. **A 381**, 17 (1982).
 - [4] F. Family and T. Vicsek, J. Phys. **A 18**, L75 (1985).
 - [5] M. Kardar, G. Parisi and Y.-C. Zhang, Phys. Rev. Lett. **56**, 889 (1986).
 - [6] *Kinetic roughening of growing surfaces*, in *Solids far from equilibrium*, edited by C. Godrèche, Cambridge University Press, U.K. (1991).
 - [7] A.-L. Barabási and H. E. Stanley, *Fractal Concepts in Crystal Growth* (Cambridge University Press, Cambridge, 1995).
 - [8] J. Krug, Adv. Phys. **46**, 139 (1997).
 - [9] B. Schmittmann and R. K. P. Zia, *Statistical mechanics of driven diffusive systems*, in *Phase transitions and critical phenomena*, edited by C. Domb and J. L. Lebowitz, vol. 17, Academic Press, New York (1995).
 - [10] J. Marro and R. Dickman, *Nonequilibrium Phase transitions in Lattice Models*, Cambridge University Press, Cambridge (1999).
 - [11] H. Hinrichsen, Adv. Phys. **49**, 815 (2000).
 - [12] L. H. Tang, J. Physique I **3**, 935 (1993).
 - [13] D. B. Chrisey and G. K. Hubler, *Pulsed Laser Deposition of Thin Films* (John Wiley & Sons, New York, 1994).
 - [14] F. Westerhoff, L. Brendel, and D. E. Wolf, in: "Structure and Dynamics of Heterogeneous Systems", eds. P. Entel and D. E. Wolf, World Scientific, Singapore (2000); B. Hinnemann, F. Westerhoff, and D. E. Wolf, submitted to *Phase Transitions*.
 - [15] B. Hinnemann, diploma thesis (2000); B. Hinnemann, H. Hinrichsen and D. E. Wolf, in preparation.
 - [16] P. Jensen and B. Niemeyer, Surf. Sci. **384**, L823 (1997).
 - [17] N. Combe and P. Jensen, Phys. Rev. **B 57**, 15553 (1998).
 - [18] In order to make the graphs comparable, we actually reflect the curves by plotting $-\ln M/\ln I$ versus $-\ln \Theta/\ln I$.